In Situ SAXS Studies of the Structural Changes of Sepiolite Clay and Sepiolite−Carbon Composites with Temperature

G. Sandí,* R. E. Winans, S. Seifert, and K. A. Carrado

Chemistry Division, Argonne National Laboratory, 9700 South Cass Avenue, Argonne, Illinois 60439

Received July 24, 2001. Revised Manuscript Received November 21, 2001

In situ small-angle X-ray scattering (SAXS) studies have been conducted to monitor the structural changes of sepiolite clay upon heating. The samples were heated first under nitrogen to establish the temperature at which pure sepiolite folds. Then, propylene was incorporated into the sepiolite channels and carbonized in situ. SAXS results indicate that the incorporation of carbon raises the structural stability of sepiolite in that the folding temperature increases from 465 °C to near 550 °C.

Introduction

In our laboratories, disordered carbons with predictable properties have been prepared using inorganic templates containing well-defined pore sizes.[1,2] The carbons have been tested in electrochemical cells as anodes in lithium secondary batteries. They deliver high specific capacity and display excellent performance in terms of the number of cycle runs.[3] Although the performance of the clay-derived carbons is excellent, there is still a need to improve the efficiency of the synthetic process without sacrificing electrochemical performance of the resulting carbons. More recently, sepiolite, a clay whose structure consists of channels, has been used as an inorganic template to produce novel carbons useful as anodes in lithium rechargeable batteries.[4] Sepiolite is a phyllosilicate clay insofar as it contains a continuous two-dimensional tetrahedral silicate sheet. However, it differs from other clays in that it lacks a continuous octahedral sheet structure. Instead, its structure can be considered to contain ribbons of 2:1 phyllosilicate structure, with each ribbon linked to the next by inversion of SiO_4 tetrahedra along a set of Si−O−Si bonds. Figure 1 a shows a schematic diagram of the structure of sepiolite.[5] In this framework, rectangular 3.7 × 10.6 Å channels run parallel to the *x*-axis between opposing 2:1 ribbons, which results in a fibrous morphology with channels running parallel to the fiber length. Individual fibers generally range from about 100 Å to 4−5 μm in length, 100−300 Å in width, and 50−100 Å in thickness. Inside the channels are protons, coordinated water, a small number of exchangeable cations, and zeolitic water. Sepiolite is a magnesium silicate with a typical molecular formula of $Mg_4Si_6O_{15}(OH)_2 \cdot 6H_2O$. Figure 1b shows the folding of the sepiolite channels after being heated (the bound water is lost).

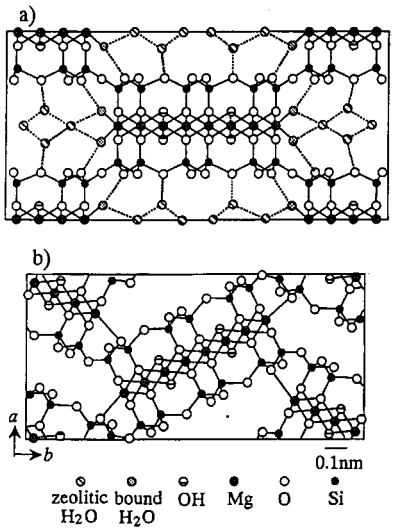

Figure 1. Schematic representation of (a) hydrated sepiolite and (b) folded sepiolite on heating. The units cells are projected on the 001 plane.

There are three sorption sites in sepiolite: (a) oxygen ions on the tetrahedral sheets, (b) a small amount of cation-exchange sites (0.1−0.15 mequiv/100 g), and (c) SiOH groups along the fiber axis. Adsorption is also influenced by the size, shape, and polarity of the molecules involved. Neither large molecules nor those of low polarity can penetrate the channels, though they can be adsorbed on the external surface, which accounts for 40−50% of the total surface area.[6] The SiOH groups act as neutral adsorption sites suitable for organic species, and the content for the Vallecas sepiolite is

* To whom correspondence should be addressed: Phone: (630) 252-1903. Fax: (630) 252-9288. E-mail: gsandi@anl.gov.

(1) Sandí, G.; Winans, R. E.; Carrado, K. A. *J. Electrochem. Soc.* **1996**, *143*, L95.
(2) Sandí, G.; Carrado, K. A.; Winans, R. E.; Brenner, J. R.; Zajac, G. W. *Mater. Res. Soc. Symp. Proc., Macroporous Microporous Mater.* **1996**, *431*, 39.
(3) Sandí, G.; Winans, R. E.; Carrado, K. A.; Johnson, C. S.; Thiyagarajan, P. *J. New Mater. Electrochem. Syst.* **1998**, *1*, 83.
(4) Sandí, G.; Carrado, K. A.; Winans, R. E.; Johnson, C. S.; Csencsits, R. *J. Electrochem. Soc.* **1999**, *146*, 3644.
(5) Inagaki, S.; Fukushima, Y.; Miyata, M. *Res. Chem. Intermed.* **1995**, *21* (2), 167.
(6) Galan, E. *Clay Miner.* **1996**, *31*, 443.

10.1021/cm010627w CCC: $22.00
Published on Web 01/12/2002

about 0.60 mmol/g.[7] These factors are all important to the goal of loading the clay with certain organic monomers that will polymerize in the channels and, following a pyrolysis step, carbonize to a material suitable for use as a carbonaceous anode in secondary lithium batteries.

Lithium ion secondary batteries are currently the best portable energy storage device for the consumer electronics market. The recent development of the lithium ion secondary batteries has been achieved by the use of selected carbon and graphite materials as an anode. The performance of lithium ion secondary batteries, such as the charge/discharge capacity, voltage profile, and cyclic stability, depend strongly on the microstructure of the anode materials made of carbon and graphite. Because of the contribution of the carbon materials used in the anode in the last five years, the capacity of the typical Li ion battery has been improved 1.7 times. However, there are still active investigations to identify the key parameters of carbons that provide the improved anode properties, as carbon and graphite materials have large varieties in the microstructure, texture, crystallinity, and morphology, depending on their preparation processes and precursor materials as well as various forms such as powder, fibers, and spherule. There is a strong correlation between the microstructural parameters and electrochemical properties of conventional and novel types of carbon materials for Li ion batteries, namely, graphitizable carbons such as milled mesophase pitch-based carbon fibers, polyparaphenylene-based carbon heat-treated at low temperatures, boron-doped graphitized materials, and templated carbons.

It is the objective of this paper to follow the structural changes of the sepiolite in situ upon heating under an inert atmosphere and upon incorporation of a polymeric matrix derived from propylene.

Methods and Materials

The sepiolite we used was from Yunclillos (Toledo, Spain), provided by TOLSA, S.A., with a BET surface area of 225 m^2/g. Propylene was obtained from AGA at 99.95% purity. X-ray powder diffraction (XRD) patterns of sepiolite were determined using a Rigaku Miniflex, with Cu Kα radiation and a NaI detector at a scan rate of 0.5° 2θ/min.

In situ small-angle X-ray scattering (SAXS) was carried out at the Advanced Photon Source, (Basic Energy Sciences Synchrotron Research Center CAT), Argonne National Laboratory. The SAXS intensity of the investigated material $I(q)$ is the function of the angle of scattering (2θ) and the wavelength (λ) of the applied radiation. This relation can be expressed as $q = 4\pi \sin \theta/\lambda$. Monochromatic X-rays (16 keV) are scattered off the sample and collected on a 15 × 15 cm^2 CCD camera. The scattered intensity has been corrected for absorption and instrument background. The differential scattering cross section has been expressed as a function of the scattering vector q. The value of q is proportional to the inverse of the length scale ($Å^{-1}$). The instrument was operated with a sample-to-detector distance of 780 mm to obtain data at $0.04 < q < 1.0$ $Å^{-1}$. For these studies, a specially designed sample holder was used to heat up the sample and collect SAXS data at the same time. Figure 2 shows a diagram of the sample holder. Sepiolite powder was inserted into a 1 mm diameter quartz capillary tube. At the bottom of the tube, a piece of quartz wool was placed to prevent the powder from falling off and to allow for the gas to flow through. The capillary tube was then inserted into the specially designed glass furnace which has an opening for the gas connection. The furnace temperature program was set up to ramp from room temperature to 700 °C at 5 °C/min and the gas flow of nitrogen or propylene was started. All of the temperature readings have an error of ±5 °C associated with them. SAXS data were collected every minute. An empty capillary was used as the blank and all the SAXS data were corrected accordingly.

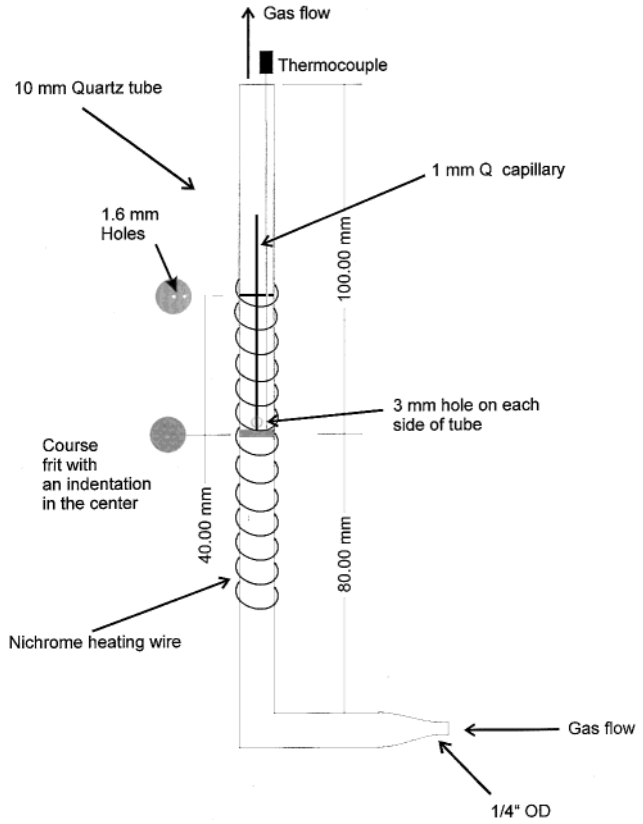

Figure 2. Schematic diagram of sample holder used in the in situ SAXS studies.

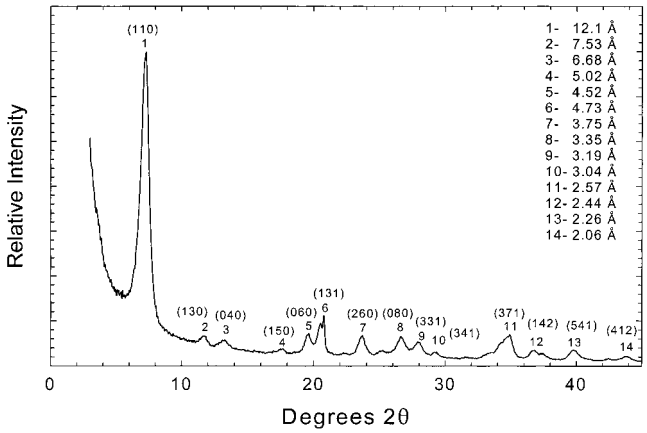

Figure 3. X-ray powder diffraction of a sepiolite sample. The inset shows the major diffraction peaks.

Results and Discussion

Several authors[6,8] have found that, between 200 and 400 °C, a sharp decrease in surface area is observed for pure sepiolite that is due to crystal folding (see Figure 1b). Studying the structural dependence of sepiolite

(7) Mehrotra, V.; Giannelis, E. P. *Mater. Res. Soc. Symp. Proc., Polym. Based Mol. Compos.* **1990**, *171*, 39.

(8) Rytwo, G.; Nir, S.; Margulies, L.; Casal, B.; Merino, J.; Ruiz-Hitzky, E.; Serratosa, J. M. *Clays Clay Miner.* **1998**, *46*, 340.

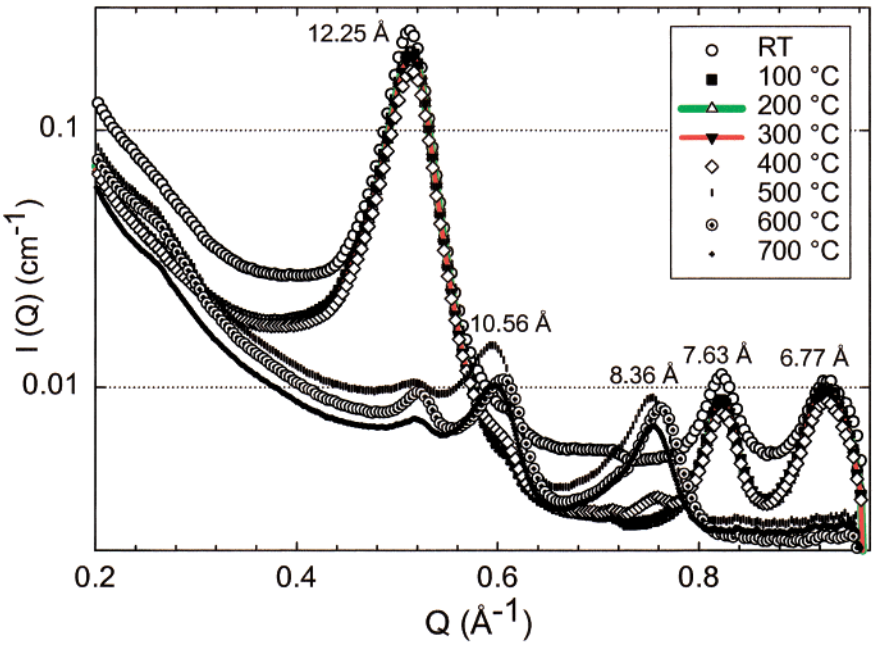

Figure 4. In situ SAXS of a sepiolite sample heated under a nitrogen flow. The heating rate was 5 °C/min. The data were collected every minute, but only one in eight (12.5%) points are shown for clarity.

upon heating is crucial in predicting and understanding the properties of the resulting carbon. In situ SAXS is an excellent technique for deriving such information because of our instrument's time-resolving capability and its high flux.

Figure 3 shows an X-ray powder diffraction pattern of a sepiolite sample showing the reflections up to 45° 2θ. The assignment of the peaks was made as per Brindley.[9] To compare with the reflections obtained in the SAXS in situ experiments, the reflections are also shown in units of Angstroms in the figure inset.

Figure 4 shows the SAXS data obtained as a function of temperature upon heating a sepiolite sample under a flow of nitrogen gas. At 25 °C, the reflections of the predominant peaks occur at 12.25 Å (110), 7.63 Å (130), and 6.77 Å (040). There are no drastic structural changes upon heating to 400 °C. Beyond 400 °C, however, the intensity of the 110 peak is greatly reduced and two new peaks appear, one at 10.56 Å and the other at 8.36 Å. At temperatures higher than 600 °C, the intensity of the peaks at 7.63 and 6.77 Å is reduced to background levels. Figure 5 shows high-resolution data taken in the temperature range between 400 and 510 °C. Notice in the figure inset that the major change occurs at 487 °C where the intensity of the peak at 10.56 Å increases. Ruiz et al.[10] found using XRD that the folding of sepiolite starts at 390 °C. Serna et al.[11] found in their XRD study that the same phenomenum occurs at ≈300 °C. It is important to point out, however, that those studies were conducted ex situ. The samples were heated and later X-ray powder diffraction spectra were taken. The risk of water adsorption in the sample is completely avoided in our experimental setup and data collection. On the basis of our results, the structure of

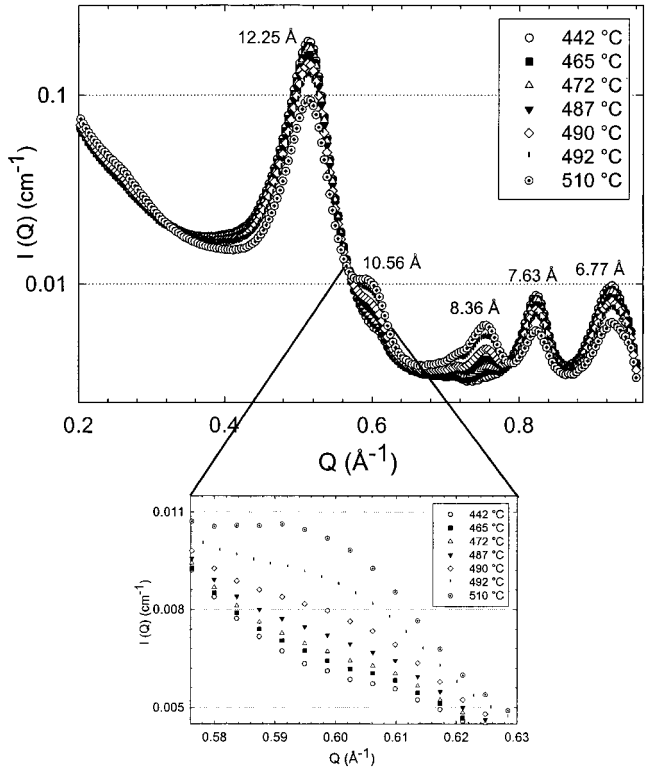

Figure 5. In situ SAXS data of a sepiolite sample heated under nitrogen (same conditions as in Figure 4). The inset shows the temperature at which the folding of sepiolite occurs.

sepiolite upon heating in nitrogen changes in three stages: (a) the zeolitic water is removed below 400 °C with no appreciable changes in the structure; (b) the bound water is lost at 400−600 °C and the structure of sepiolite folds at 487 °C; (c) the hydroxyl water disappears above 600 °C, as evidenced by the loss of the peaks at 7.63 and 6.77 Å.

Figure 6 shows in situ SAXS data of the incorporation and polymerization of propylene in the sepiolite channels. Overall peak positions are similar to the N_2 case.

(9) Brindley, A. *Am. Miner.* **1959**, *44*, 495.
(10) Ruiz, R.; del, Moral, J. C.; Pesquera, C.; Benito, I.; Gonzalez, F. *Thermochim. Acta* **1996**, *279*, 103.
(11) Serna, C.; Ahlrichs, J. L.; Serratosa, J. M. *Clays Clay Miner.* **1975**, *23* (6), 452.

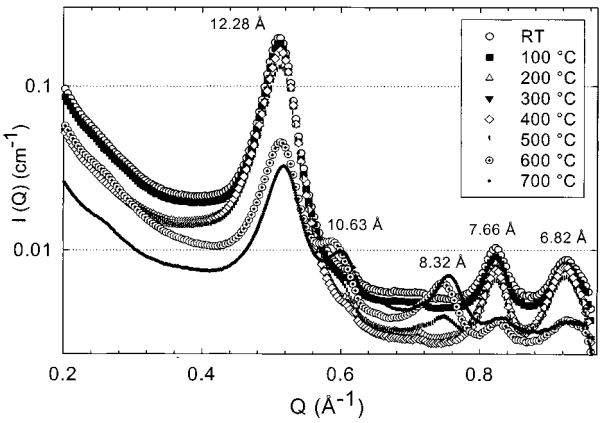

Figure 6. In situ SAXS of a sepiolite sample heated under a propylene flow. The heating rate was 5 °C/min. The data were collected every minute, but only one in eight (12.5%) points are shown for clarity.

However, a critical difference occurs in the temperature at which the structural changes occur. For example, the intensity of the (110) reflection at 12.28 Å decreases the most between 500 and 600 °C, as opposed to between 400 and 500 °C when the clay is heated under nitrogen. In addition, the intensity of this reflection does not go to background levels when the temperature reaches 700 °C. A closer look into the temperature ranges between 500 and 600 °C (Figure 7) indicates that most of the intensity is lost between 525 and 547 °C. The incorporation of propylene in the channels of sepiolite therefore delays the folding of the structure by as much as 60 °C. Also, the sepiolite structure remains largely intact as evidenced by the presence of the peaks at 12.28, 7.66, and 6.82 Å up to 700 °C. This indicates that the carbon is present within the sepiolite channels and stabilizes the structure.

Conclusions

In situ SAXS studies showed that folding of sepiolite channels occurs at about 487 °C, a significantly higher temperature than previously reported[10,11] via X-ray powder diffraction, where the sample was heated and later the spectra were taken. The incorporation of propylene in the channels of sepiolite delays the folding of the structure by 90 °C. This indicates the existence of a stable clay−carbon composite phase. Polymerization and carbonization takes place and, upon removal of the clay, a carbon is obtained whose electrochemical properties have been tested as described in detail by Sandí et al.[4,12]

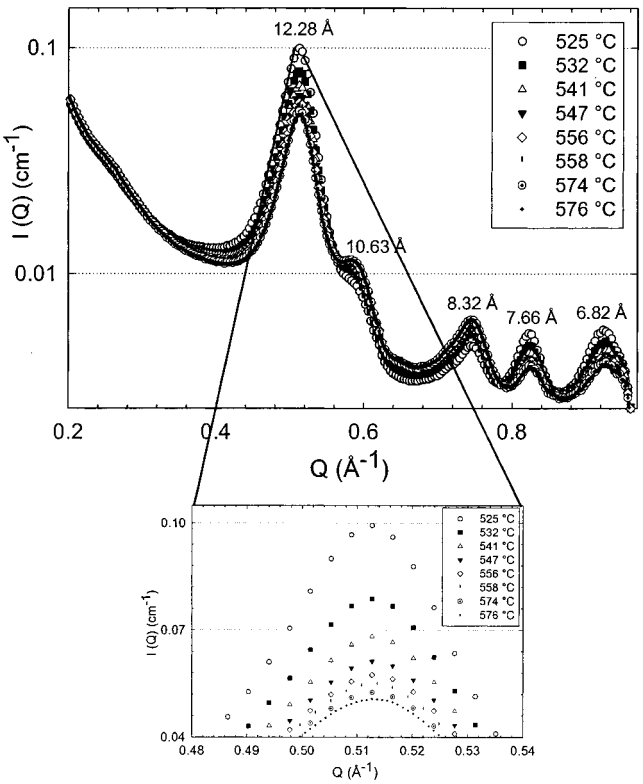

Figure 7. In situ SAXS data of a sepiolite sample heated under propylene (same conditions as in Figure 6). The inset shows the temperature at which the folding of sepiolite occurs (about 60 °C higher than when heated under nitrogen).

Acknowledgment. Use of the Advanced Photon Source was supported by the U.S. Department of Energy, Office of Science, Office of Basic Energy Science, under Contract W-31-109-ENG-38. Support from BESS-RC-CAT personnel is greatly appreciated. This work was performed under the auspices of the U.S. Department of Energy, Office of Basic Energy Sciences, Division of Chemical Sciences, under Contract W-31-109-ENG-38.

CM010627W

(12) Sandí, G.; Winans, R. E.; Carrado Gregar, K. U.S. Patent 6110621, 2000.